Gating of Cardiac Na^+ Channels in Excised Membrane Patches after Modification by α-Chymotrypsin

Carmen Valenzuela* and Paul B. Bennett, Jr.
Department of Pharmacology, Vanderbilt University School of Medicine, Nashville, Tennessee 37232 USA

ABSTRACT Single cardiac Na^+ channels were investigated after intracellular proteolysis to remove the fast inactivation process in an attempt to elucidate the mechanisms of channel gating and the role of slow inactivation. Na^+ channels were studied in inside-out patches excised from guinea-pig ventricular myocytes both before and after very brief exposure (2–4 min) to the endopeptidase, α-chymotrypsin. Enzyme exposure times were chosen to maximize removal of fast inactivation and to minimize potential nonspecific damage to the channel. After proteolysis, the single channel current-voltage relationship was approximately linear with a slope conductance of 18 ± 2.5 pS. Na^+ channel reversal potentials measured before and after proteolysis by α-chymotrypsin were not changed. The unitary current amplitude was not altered after channel modification suggesting little or no effect on channel conductance. Channel open times were increased after removal of fast inactivation and were voltage-dependent, ranging between 0.7 (−70 mV) and 3.2 (−10 mV) ms. Open times increased with membrane potential reaching a maximum at −10 mV; at more positive membrane potentials, open times decreased again. Fast inactivation appeared to be completely removed by α-chymotrypsin and slow inactivation became more apparent suggesting that fast and slow inactivation normally compete, and that fast inactivation dominates in unmodified channels. This finding is not consistent with a slow inactivated state that can only be entered through the fast inactivated state, since removal of fast inactivation does not eliminate slow inactivation. The data indicate that cardiac Na^+ channels can enter the slow inactivated state by a pathway that bypasses the fast inactivated state and that the likelihood of entering the slow inactivated state increases after removal of fast inactivation.

INTRODUCTION

Current through voltage gated Na^+ channels drives the upstroke of the cellular action potential and in cardiac cells this supports electrical conduction initiating the excitation-contraction coupling process (Brown et al., 1981; Fozzard et al., 1985; Fozzard and Hanck, 1992; Catterall, 1986; Catterall, 1988). It is generally accepted that Na^+ channels exist in at least three primary classes of kinetically defined states: closed (but available to open), open and inactivated (closed but not available to open). The mechanisms of Na^+ channel gating and the relationship between Na^+ channel activation and inactivation have been the focus of considerable investigational effort (Hodgkin and Huxley, 1952; Goldman and Schauf, 1972; Armstrong and Bezanilla, 1977; Bezanilla and Armstrong, 1977; Gillespie and Meves, 1980; Bean, 1981; Patlak and Horn, 1982; Oxford, 1981; Vandenberg and Horn, 1984; Gonoi and Hille, 1987). Understanding gating mechanisms is especially important for cardiac Na^+ channels in order to understand mechanisms of antiarrhythmic drug action. Differences between neuronal and cardiac Na^+ channels have been noted at both the functional and molecular levels (Kirsch and Brown, 1989; Noda et al., 1984; Noda et al., 1986; Rogart et al., 1989). Although it is generally accepted that Na^+ channels can inactivate from both closed and open states, the importance of these two pathways of inactivation are different in heart and nerve (Lawrence et al., 1991; Berman et al., 1989; Aldrich et al., 1983). Studies of mammalian neuronally derived, TTX-sensitive Na^+ channels in GH_3 pituitary cells (Gonoi and Hille, 1987) and N18 neuroblastoma cells (Cota and Armstrong, 1989) have revealed a marked increase in sodium current and a negative shift in the conductance-voltage relationship after enzymatic removal of fast inactivation. These results support a model of Na^+ channel inactivation developed by Aldrich et al. (1983). Their model states that voltage-independent inactivation is strongly coupled to activation and it occurs from both open and closed states of the channel. Their data showed that neuronally derived channels usually opened only once before "irreversibly" entering the inactivated state. Data derived from cardiac Na^+ channels suggest that this model is not appropriate (Kunze et al., 1985; Yue et al., 1989). Cardiac channels have a greater tendency to reopen at membrane potentials between −60 and −30 mV. In addition, the voltage dependence of cardiac Na^+ channel open times has been controversial. Nilius (1988) has concluded that the open times were not voltage dependent, whereas Grant and Starmer (1987), Scanley et al. (1990), and Lawrence et al. (1991) have provided evidence that they are voltage-dependent. An important goal for cardiac ion channel biophysics is to assign an appropriate state diagram for channel gating and to begin to determine individual rate constants. Our approach toward this goal has been to try and simplify the channel gating by eliminating certain transitions.

In addition to fast inactivation, a much slower gating processes exists which has been referred to as slow inactivation (Rudy, 1978; Rudy, 1981; Saikawa and Carmeliet, 1982;

Received for publication 19 January 1994 and in final form 28 April 1994.

Address reprint requests to Paul B. Bennett, Ph.D., CC-2209 Medical Center North, Vanderbilt University School of Medicine, Nashville, TN 37232-2171. Tel.: 615-322-4836; Fax: 615-322-7186.

Dr. Valenzuela's present address: Department of Pharmacology, School of Medicine, Universidad Complutense, 28040 Madrid, Spain.

0006-3495/94/07/161/11 $2.00

Gintant et al., 1984; Clarkson et al., 1984; Patlak and Ortiz, 1985; Quandt, 1987). A number of observations suggest the importance of slow inactivation in cardiac cells: 1) it may mediate suppressed excitability in regions that are depolarized for prolonged periods (ischemia); 2) certain agents that suppress cardiac excitability bind relatively selectively to slow inactivated Na^+ channels; 3) Na^+ channels that inactivate slowly may maintain the action potential plateau. Nevertheless, there is little or no information on mechanisms of slow inactivation at the single channel level for cardiac Na^+ channels. Is slow inactivation in heart a separate and independent process from fast inactivation? Is the slow inactivated state entered by way of the fast inactivated state?

In an effort to better understand mechanisms of gating in cardiac Na^+ channels including both fast and slow inactivation, we have utilized single channel recordings from excised membrane patches where fast inactivation was removed by very brief exposure of the cytoplasmic surface to the endopeptidase, α-chymotrypsin. Excised patches permitted very brief exposures to the enzyme to minimize damage to less accessible protein domains. The removal of inactivation by peptide cleaving enzymes may have advantages over toxins that slow the inactivation process, especially for subsequent pharmacological studies of open channel block where there is a potential for interactions between drugs and toxin.

MATERIALS AND METHODS

Cell isolations

Ventricular myocytes were obtained from 200- to 250-g guinea pigs by standard collagenase dispersion (Farmer et al., 1983; Valenzuela and Bennett, 1991). Hearts were mounted on a Langerdorff apparatus and perfused with a nominally calcium-free Joklik medium for 3 min, followed by a 10-min perfusion with Joklik medium containing also 0.06% collagenase (153 U/mg; Worthington, type 2, Freehold, NJ), 0.02% trypsin (GIBCO, Grand Island, NY) and 50 μM $CaCl_2$. The hearts were then minced and gently agitated in a high potassium (KB) solution (Isenberg and Klöckner, 1982). Cells were washed three times in KB media and stored in this solution for 2 h at room temperature. The cells were then transferred to an enriched medium 199 (Sigma Chemical Co., St. Louis, MO) and maintained in an incubator at 37°C. Only rod-shaped cells with clear cross-striations in a 1.8 mM Ca^{2+} solution were used. The isolated cells were transferred to a 0.5-ml chamber mounted on the stage of an inverted microscope for voltage clamp studies.

Solutions

The cells were superfused at 1 ml/min with a Tyrode solution of the following composition (mM): NaCl, 145; $CaCl_2$, 1.8; $MgCl_2$, 1.0; KCl, 4.0; glucose, 10; HEPES, 10; titrated to pH 7.35 with NaOH. The patch electrode was filled with a solution containing (mM): NaCl, 145; $MgCl_2$, 2.0; $CaCl_2$, 0.1; HEPES, 10; titrated to pH 7.35 with NaOH. After establishment of a gigaohm seal the bath solution was changed to a solution containing (mM): NaF, 10; CsF, 110; CsCl, 20; $MgCl_2$, 2.0; EGTA, 2; HEPES, 10; titrated to pH 7.35 with CsOH. α-Chymotrypsin (type VII, TLCK-treated to avoid trypsin activity, Sigma) was dissolved in a solution containing (mM): CsCl, 80; CsF, 80; EGTA, 10; HEPES, 10; titrated to pH 7.35 with CsOH.

Patch clamp recordings

All experiments were done at room temperature (22°C). The inside-out configuration of the patch-clamp method (Hamill et al., 1981) was used. Recordings were made with an Axopatch-1C patch clamp amplifier (Axon Instruments, Burlingame, CA). Patch pipettes were constructed from starbore capillary tubes (Radnoti Glass Technology, Monrovia, CA) and heat polished after being coated near the tip with a hydrophobic polymer (Sylgard, Dow Corning). Electrodes with resistances of 5–10 MΩ were used.

Membrane patches were excised by lifting a cell from the bottom of the bath into a jet of solution. The force of this stream of solution removed the cell from the pipette leaving an excised inside-out patch. After collection of control data, the excised patch was briefly exposed to α-chymotrypsin (0.4 mg/ml; TLCK-treated, Sigma). The exposure was terminated when Na^+ channels failed to inactivate during a strong depolarization (0 mV). This effect was obtained in 2–5 min and the enzyme solution was then replaced with the standard internal solution described above.

Voltage-clamp command pulses were generated by a 12-bit digital-to-analog converter. Membrane currents were filtered at 2 kHz (−3 dB) by a four-pole Bessel filter before sampling at 20 kHz by a 12-bit analog-to-digital converter. In specific experiments data were filtered at 5 kHz before sampling. This was done in an attempt to reduce the number of missed brief closures at the lower filter setting. The majority of data were collected with a 2-kHz filter. The differences in open times with these filter settings occurred for open times <200 μs and we usually excluded these brief openings from our analysis. Therefore, the state lifetimes reported may be distorted by omission of these events. Sampled data were stored on the hard disk of a microcomputer for later analysis. No corrections were made for electrode junction potentials which were less than 3 mV. Pulse protocols were generally delivered once every 5 s unless indicated otherwise and the standard holding potential was −120 mV. The standard test pulse duration as 50 ms unless indicated otherwise.

Data analysis

Capacitative and linear leakage currents were subtracted by averaging the traces without activity and subtracting the averaged "null" from each trace. Data were analyzed with custom software written in BASIC (Microsoft, QuickBASIC) using an event detection scheme based on a half-amplitude criterion as described by Colquhoun and Sigworth (1983). Single channels recordings were first analyzed by generation of amplitude histograms which allowed identification of current levels associated with channel openings. Amplitude histograms were fitted with Gaussian curves using a simplex algorithm. The mean and standard deviation (SD) of the all points current amplitude histograms were then used in further analysis of open and closed durations. Fig. 1 illustrates this approach. In the analysis of openings, we noted occasional openings or closing to what appeared to be a substate level. Since these events were rare, we did not segregate them in the analysis and any such openings or closings were considered to be full openings or closings.

Open channel probabilities were calculated by dividing the ensemble average current by the product of the unitary current (obtained from amplitude histograms) and the number of Na^+ channels in the patch. The number of channels in a patch was estimated by a binomial analysis (Patlak and Horn, 1982) and from the maximum number of overlapping events at the beginning of a voltage step. The mean open times were determined by averaging the open times list obtained as described above or by fitting an exponential function to the binned distribution of open times. Patches with more than three channels were not used for determining lifetime histograms, and only patches with one channel were used for latency analysis. Analysis of simulated data indicated that our programs could reliably register the open times when three or fewer channels were in a patch. Closed times were estimated by fitting sums of exponentials to the observed closed time distributions. Ensemble average currents were usually obtained from 96 and 128 sweeps. Results are expressed as mean and standard errors where appropriate or as indicated in the figure legends.

RESULTS

The activity of Na^+ channels and corresponding ensemble averages recorded from an excised patch at a transmembrane

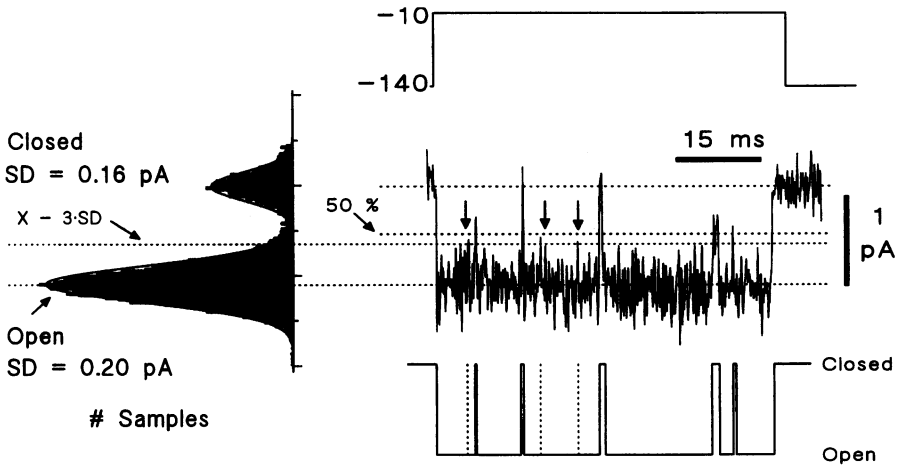

FIGURE 1 Measurement of single channel current amplitudes by all points amplitude histograms. The voltage protocol is indicated. Upon stepping the membrane potential to −10 mV, a chymotrypsin modified Na^+ channel began opening. The digitized current samples were sorted into bins to form histograms (*left*) of current levels. Histograms show open and closed distributions from records in addition to the one shown. Gaussian curves (*solid lines*) were fitted to the distributions to obtain a means and standard deviations. Beneath the raw current tracing is a computer generated reconstruction of the opening and closing of the channel. The solid line was obtained from a 50% criterion; the additional closures (*dotted lines*) were obtained using a 3-SD excursion criterion (see Materials and Methods).

potential of −30 mV are shown in Fig. 2. The channel activities before (*control, A*) and after (*B*) enzymatic modification are shown. In the control records (*A*) most of the openings of the Na^+ channel appear at the beginning of the depolarizing step. Reopenings were few and long-lasting bursts of openings were absent. The ensemble averaged Na^+ current reaches a peak and inactivates in <10 ms.

Fig. 2 *B* shows records obtained after covalent modification of channels by α-chymotrypsin. The openings of the modified channel were longer and reopenings were more common than in the control consistent with successful removal of the fast inactivation process. The single channel open amplitudes were similar in control and after treatment with the enzyme, suggesting that the conductance of the channel was not modified by α-chymotrypsin.

Single channel conductance

We estimated the single channel current amplitude by sorting the digitized records into "all points" histograms. Current amplitude histograms obtained at three different membrane potentials after proteolysis are shown in Fig. 3. These form distributions around the major current levels. For different voltage steps, the distributions corresponding to the open channel shift on the *x*-axis due to changes in driving force for Na^+ through the channel.

Fig. 4 *A* shows mean single channel current obtained from amplitude histograms as a function of membrane potential (i-V) before and after channel modification by α-chymotrypsin. The extrapolated reversal potential and the conductance of the channel were similar. Under the conditions used in these experiments, the equilibrium potential predicted by the Nernst equation is +68 mV. The extrapolated reversal potential determined from a linear approximation by least squares regression of the data in control and after covalent modification by α-chymotrypsin was predicted by the Nernst relationship within the limits of measurement error. The single channel slope conductance was 16.3 ± 1.9 pS in control and 18.1 ± 2.5 pS (NS; n = 15) after covalent modification with α-chymotrypsin. These slope conductance

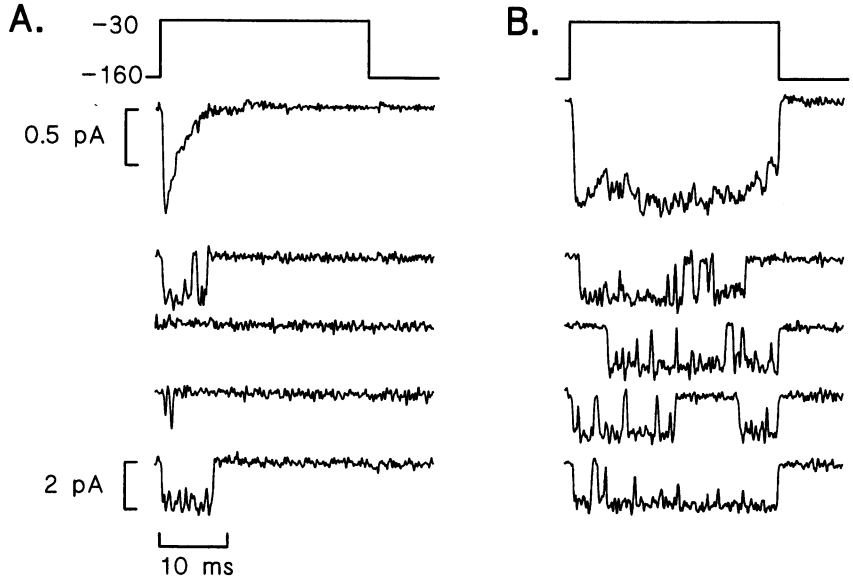

FIGURE 2 Single Na^+ channel currents and ensemble averages in an inside-out patch in control (*A*) and after removal of fast inactivation (*B*). The patch was held at −160 mV for 1 s between pulses to −30 mV.

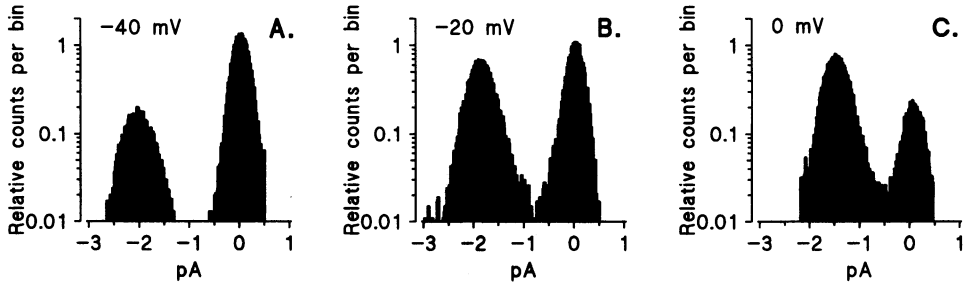

FIGURE 3 Current amplitude histograms obtained after removal of inactivation with α-chymotrypsin. Histograms recorded at three different test potentials are shown: −40 (*A*), −20 (*B*), and 0 mV (*C*). The holding potential was −140 mV. The closed channel mean (peak) is centered near 0 pA, and the open channel peaks shift right for larger voltage steps as the driving force ($E_{Test} - E_{Na}$) for current through the channel decreases.

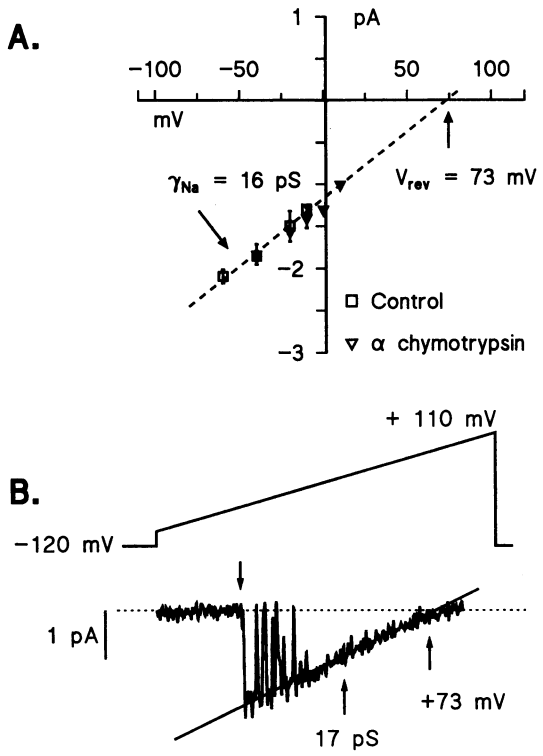

FIGURE 4 (*A*) Current-voltage (i-V) relationships in control and after (Δ) removal of inactivation. Data are means obtained from 6 experiments with 2 times the SEM indicated in each direction. The dashed line has a slope of 16 pS and an *x*-intercept (reversal potential) of +73 mV. (*B*) Current-voltage relationship obtained by ramping the clamp voltage from −90 to +110 mV in a channel with inactivation removed. As the ramp voltage passed −60 mV the channel began to open and flicker closed. Brief outward openings can be observed beyond the reversal potential. The line through the data has a slope of 18 pS.

estimates are similar to those previously described (Kunze et al., 1985; Berman et al., 1989) and suggest that α-chymotrypsin did not significantly alter the permeation properties of the channel under the conditions employed here.

We further investigated the effects of α-chymotrypsin on the single channel conductance using voltage clamp ramps. This allowed a direct estimate of the reversal potential of the Na^+ current and the single channel conductance over a range of membrane potentials. These measurements were not possible for channels with fast inactivation intact. Fig. 4 *B* shows single α-chymotrypsin-modified Na^+ channel current during such a voltage ramp. Upon ramping the membrane potential from −90 to +110 mV, the channel began opening at potentials positive to −60 mV. During a ramp the channel would sometimes close and then reopen. The slope conductances estimated by fitting a linear function to the data excluding the closures gave similar values to those obtained from the amplitude histograms. These data suggest that the reversal potential was not changed by these brief exposures to the enzyme. Attempts to fit the data with the Goldman-Hodgkin-Katz current equation (see Hille, 1992) were unsuccessful. This equation produced too much rectification which suggests that another permeation model may be more appropriate.

Voltage-dependent gating of α-chymotrypsin modified channels

Under control conditions, open durations of Na^+ channels became slightly longer between −40 and 0 mV and a channel typically opened fewer than two times before inactivating. At more negative membrane potentials (between −70 and −50 mV) open times were briefer and channels were more likely to open, close and reopen repeatedly. After removal of fast inactivation, the voltage dependence of the open times did not change qualitatively: open times increased with depolarization and reopenings were more common at more negative potentials. This behavior was analyzed in more detail by creating open and close duration histograms from openings obtained at different membrane potentials. Fig. 5 shows the distribution of open times at two different step potentials (−20 and 0 mV). Also shown are the superposition of fitted exponential functions which gives the mean of the distribution and shows that the majority of openings were accounted for by a single open state. The average open time at −10 mV was 3.2 ± 0.55 ms (n = 6). The use of two exponentials, as would be necessary for two open states, did not improve the fit.

Open times as a function of membrane potential are summarized in Fig. 6 (*top*). The open times were relatively short at negative step potentials (<−50 mV) and increased with

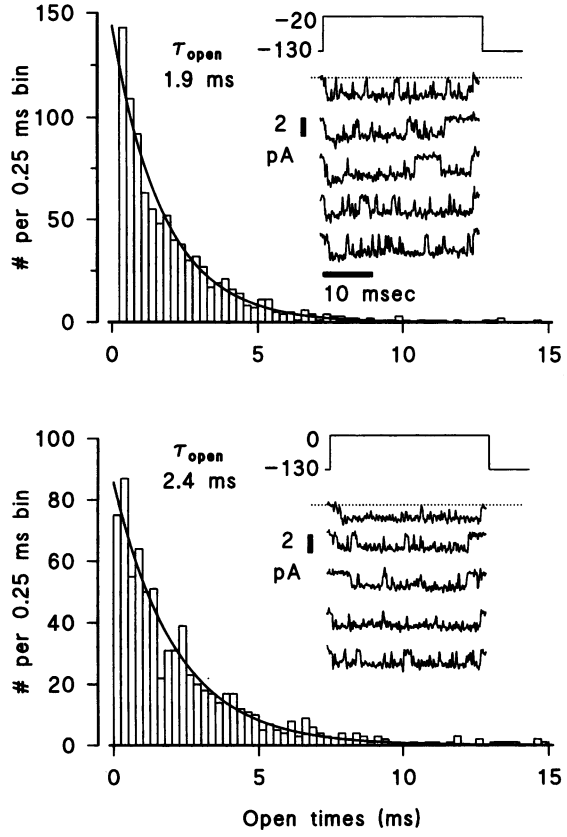

FIGURE 5 Open time histograms of modified Na^+ channels at two different membrane potentials: −20 and 0 mV. Channel open durations were sorted into 0.25-ms bins and the number of opening durations falling into each bin are shown. The line superimposed on each histogram represents the fit of an exponential distribution (one open state) with the means of the distributions (τ_{open}) indicated in the figure. The insets show individual records of channel openings at these membrane potentials. Open times increased with depolarization over the range of membrane potentials between −70 mV up to −10 mV.

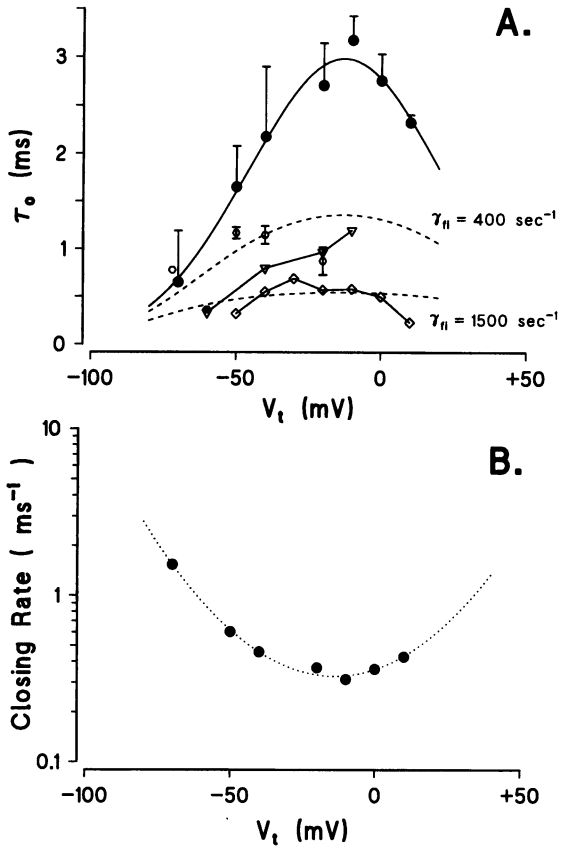

FIGURE 6 (*A*) Relationship between the mean open times and the test potential before (*open symbols*) and after (●) treatment with α-chymotrypsin. The *open symbols* indicate open times with fast inactivation intact. The *circles* represent means and SE of open times in 3 or more patches after removal of fast inactivation. The inverted triangles and diamonds are data from two different patches where open times could be determined over the indicated voltage range in the same patch. The *open hexagons* are averaged data from different patches with intact inactivation. ●, increase in open times after removal of fast inactivation. The open times were voltage dependent and were not a simple monotonic function of membrane potential. The *dashed curves* show the predicted open times when using the closing rate from Fig. 6 *B* and a voltage-independent inactivation rate constant of 400 or 1500/s ($\tau_{open} = \{\beta + \gamma_{fi}\}^{-1}$. (*B*) Reciprocal of the mean open times (β = closing rate) as a function of membrane potential. Values are plotted on a logarithmic ordinate and show that after this transform the relationship is not linear. The *dotted curve* is the best fit of the relationship predicted from reaction rate theory: $\Delta G = -RT \cdot \ln(\beta/\nu)$ where $\nu = \kappa \cdot kT/h$; β is the closing rate constant, R is the gas constant, k is Boltzmann's constant, T is temperature, h is Planck's constant and κ is a transmission coefficient (usually assumed to be 1). The value of ν is $\sim 6 \times 10^{12}$ s^{-1} and it is the attempt rate for crossing the barrier; it gives the upper limit for the transition frequency. The barrier heights for this transition ranged between 13 and 14 kcal/mol (+10 to −70 mV) under these conditions.

greater step potentials. At test potentials more positive than −10 mV, the observed open times decreased again. For an ion channel that behaves according to Markovian kinetics, the open lifetime of the channel is equal to the reciprocal sum of the rate constants leaving the open state. Since channels with inactivation removed were kinetically simpler than intact channels (the $O \rightleftharpoons I$ transition is eliminated), we estimated the closing rate constant as the reciprocal of the open times. We assumed that after removal of fast inactivation only one pathway exits the open state. Therefore, the reciprocal of the open time is a direct measure of this closing rate constant.

$C_n \overset{\beta}{\leftarrow} O \underset{\gamma}{\rightarrow} I_{fast}$	$C_n \overset{\beta}{\leftarrow} O$	$\beta = (\tau_{open})^{-1}$
Fast inactivation intact	Fast inactivation removed	Closing rate

Fig. 6 (*bottom*) plots the voltage dependence of this apparent rate constant and shows the predicted voltage dependence derived from reaction rate theory (Stevens, 1978) where the energy barriers separating the open and close states range between 13 and 14 kcal/mol (dashed line in Fig. 6).

Slow Na^+ channel inactivation

Following channel proteolysis we observed numerous consecutive records where no channel openings occurred. These "null records" appeared in clusters between sweeps with apparently normal opening behavior. A Runs analysis (Bendat

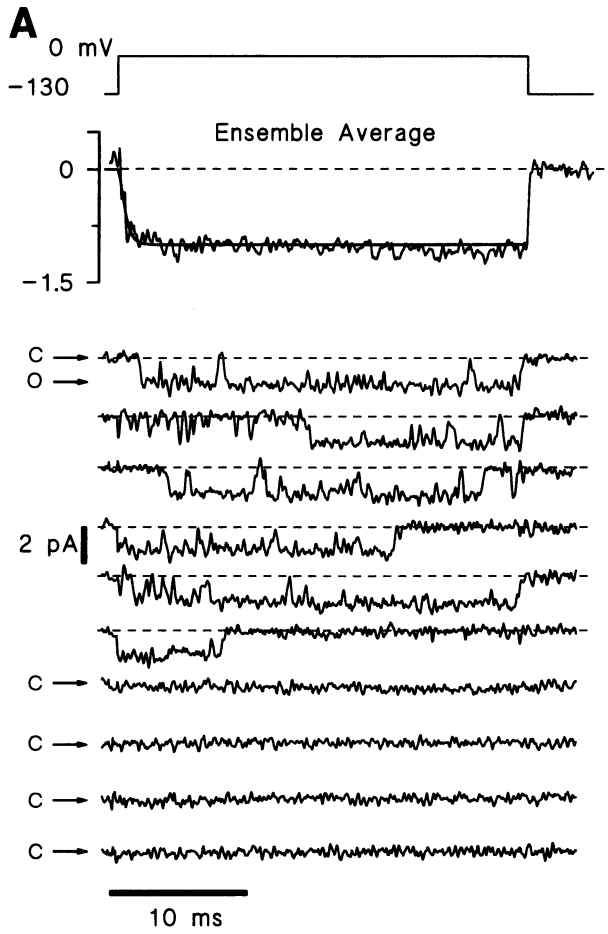

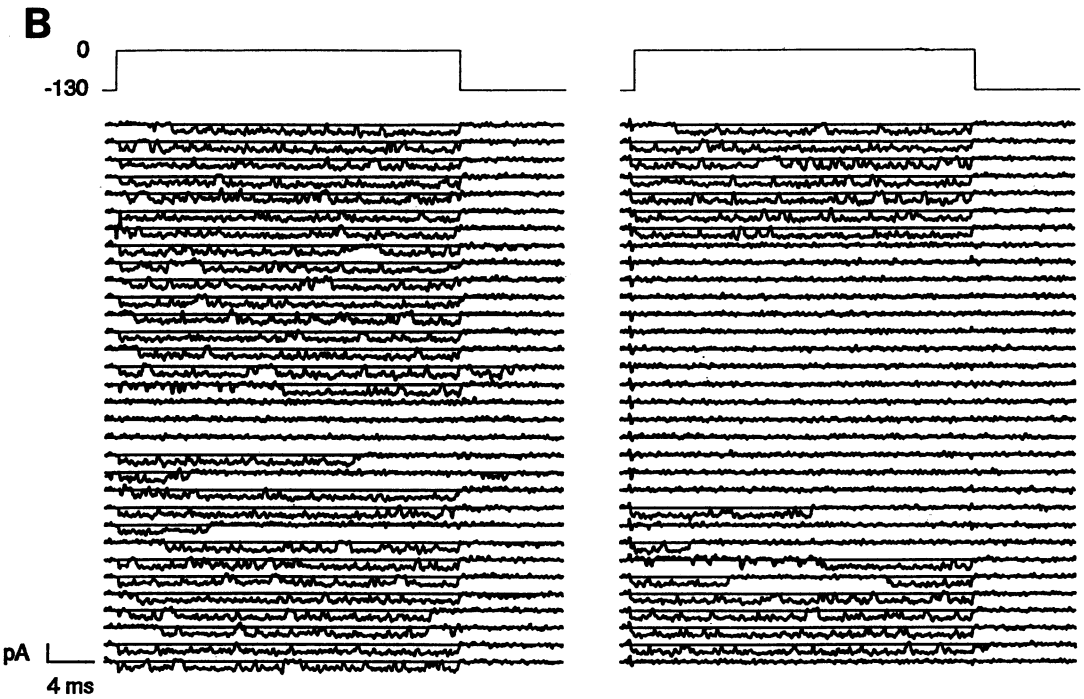

FIGURE 7 (*A*) Prolonged closed times of a channel after removal of fast inactivation. Channel openings were measured after applying a test pulse to 0 mV from a holding potential of −130 mV. The ensemble average of 96 tracings is shown along with individual records. As seen in the ensemble average, no time-dependent inactivation was observed during the voltage clamp step. Under these conditions the available channels are expected to have a high probability (near 1) of opening. Nevertheless, numerous tracings with no openings were observed as if the channel is unavailable to open. (*B*) Sixty-four consecutive records (*left bottom* to *top* to *right bottom* to *top*). Recordings were made once every 3 s, therefore 15 consecutive blank tracings represents over 45 s where the channel was unavailable to open. Note in sweep 42 (10th from bottom right) which is the last sweep with an opening before a long period without openings, the channel appears to enter the slow inactivated state from the open state.

and Piersol, 1986) on the clustering of the null records indicated that they did not occur randomly. The statistical probability of observing such a clustering was vanishingly small ($p < 0.001$). These ensembles of null records appeared to occur randomly during long periods of successive records as if the channel occasionally entered a long lived closed or inactivated state. This observation was more likely when more positive membrane potentials were applied. A

representative example of this behavior is shown in Fig. 7, which contains channel activity during a membrane potential step to 0 mV. Fig. 7 *A* shows ten consecutive sweeps. Even at this strong depolarization, numerous closings and reopenings were observed, indicating that P_{open} was not 1 at 0 mV. After closing in the sixth record the channel did not reopen for more than 10 s. Fig. 7 *B* shows a similar pattern of behavior in a recording of 64 consecutive sweeps. Note how the channel normally opens with each step depolarization, but there are long occurrences of failure to open, even though the holding potential was −130 mV and the test step was 0 mV. In sweep 42 the channel is open but then closes approximately halfway through the sweep and does not reopen in 14 additional steps over 42 s.

We tested for the voltage dependence of this apparent slow inactivation process using two different voltage clamp protocols. In one, a standard double pulse protocol was used with a 2-s conditioning pre-pulse to different membrane potentials (between −120 and +20 mV); the fraction of Na^+ channels available to open during a test pulse to −10 mV was estimated from ensemble averages. For practical reasons it was difficult to use numerous very long pre-pulses to induce slow inactivation, therefore 2-s pre-pulses were used as a compromise. Although these pre-pulses were sufficient to induce slow inactivation, a true steady state may not have been achieved. Thus, the measured slope and the midpoint of the relationship may not reflect the actual steady state partitioning into the slow inactivated state, although the errors are not expected to be large. Fig. 8 *A* shows a typical experiment using this protocol. Even when the fast inactivation was removed, a slower voltage-dependent component of inactivation was still present. The results are summarized in Fig. 8 *B*. These results were fitted using a Boltzmann equation, where the $V_{1/2}$ was −64 mV. This is much more positive than the midpoint obtained for fast inactivation in these same cells and patches (−95 to −110 mV after whole-cell dialysis or patch excision) but it is very close to the midpoint for slow inactivation reported by Rudy (1978) and Kunze et al. (1985).

In another group of experiments, a 60-s conditioning pre-pulse to 0 mV was applied before the test pulse to −40 mV. In these experiments there was a large decrease of the open probability after the long pre-pulse (Fig. 9). This decrease in open probability resulted from an increase in the fraction of null records. Fig. 9 shows an example of the behavior of the Na^+ channel, before and after channel modification with α-chymotrypsin. Current in each trace was integrated and plotted as a function of time. This display shows the open probability (fractional open time) of each sweep. On the left, the P_{open} in each sweep is shown either with or without a pre-pulse. The open probability was greatly increased after α-chymotrypsin treatment; however, a 60-s pre-pulse to 0 mV caused a large decrease in the open probability (*right*). The average P_{open} before and after removal of fast inactivation and after insertion of the pre-pulse is shown above the diary.

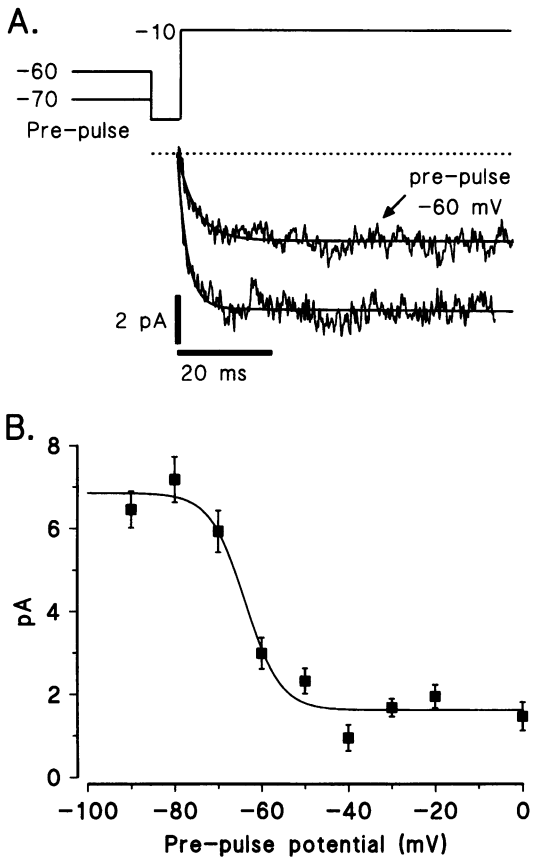

FIGURE 8 Voltage dependence of slow inactivation. (*A*) Ensemble averages of obtained from a standard two- pulse inactivation protocol. Averages were selected to show maximum inward current (pre-pulse to −70 mV) and a pre-pulse that reduced the ensemble average by ~50% (pre-pulse to −60 mV). Note the absence of any apparent time dependent inactivation during the test pulse (to −10 mV). The brief gap between the pre-pulse and test pulse was used to assure that all test pulses came from the same potential and it had no effect on the current during the test pulse. (*B*) Averaged steady-state current obtained during test pulses to −10 mV as a function of the pre-pulse voltage step. The solid curve represents the fit of a Boltzmann relationship. The membrane potential for half-maximal inactivation ($V_{1/2}$) was −64 mV and the fitted slope factor of 4.05 mV. Note that even for large pre-pulse potentials, complete inactivation did not occur.

DISCUSSION

Early work in nerve established that the fast inactivation process was eliminated by internal exposure to pronase (Armstrong et al., 1973). This lead to the hypothesis that inactivation resulted from a peptide tethered to the intracellular surface of the channel protein, and that this "peptide ball on a chain" could occlude the open pore and produce the channel inactivation. Recent evidence has implicated a cytoplasmic protein structural component that links transmembrane domains III and IV of the Na^+ channel protein in the fast inactivation process (Stühmer et al., 1989; Moorman et al., 1990; Vassilev et al., 1989; West et al., 1992). Thus, removal of fast inactivation is one strategy (Patlak and Horn, 1982) to isolate the closed-open transitions ($C \rightleftharpoons O$).

We have investigated the gating of cardiac Na^+ channels after treatment with the proteolytic enzyme α-chymotrypsin

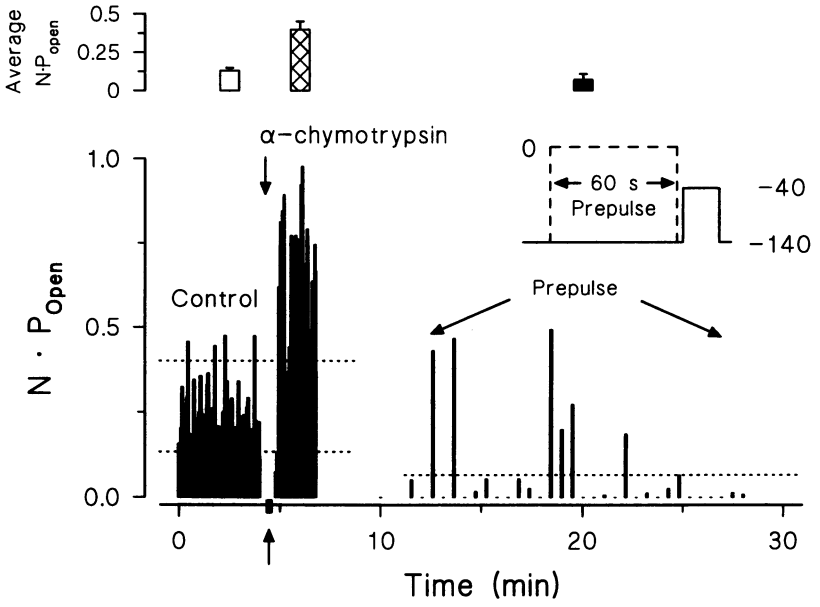

FIGURE 9 The effect of a pre-pulse on channel opening probability. (*Top*) Bar graph shows the average ± 2 SEM of $N \cdot P_{open}$ during control (before exposure to α-chymotrypsin), after removal of fast inactivation, and during a pre-pulse after removal of fast inactivation. The averages were obtained from the records shown in the diary analysis in the bottom panel. (*Bottom*) Diary of Na^+ channel activity in a patch containing three ($N = 3$) channels after removal of the fast inactivation. The fractional open time ($N \cdot P_{open}$) in each record is plotted as a function of time during the experiment. Each vertical bar represents a recording during a voltage jump to −40 mV. α-Chymotrypsin was applied and washed out during the time indicated by the arrow and the box on the *x*-axis. The means of each group of tracings are also shown by the dotted lines and are shown in the bar graph in the top panel. A pre-pulse to 0 mV reduced the likelihood of channel opening during the voltage jump to −40 mV.

in an attempt to remove fast inactivation. The simplest interpretation of our data is that α-chymotrypsin proteolysis cleaves a part of the channel protein that normally causes fast inactivation, resulting in removal of fast inactivation. This interpretation is consistent with the original data supporting an intracellular part of the channel protein that can block conduction. It is also consistent with the recent mutagenesis data demonstrating that the III-IV interdomain, a presumed intracellular loop, is intimately involved with fast inactivation. This is the interpretation we favor. An alternative interpretation is that α-chymotrypsin causes a slowing of normal fast inactivation. However, even in this case, our interpretation (see below) regarding the higher order dependence of the closing rate on membrane potential is still valid as discussed in detail below.

The main results of this study were: 1) the conductance of enzymatically modified Na^+ channels were not significantly altered; 2) open times in modified Na^+ channels were increased relative to control which is consistent with removal of a kinetic pathway out of the open state; 3) the open times were voltage-dependent; 4) channels with fast inactivation removed retained a slower inactivation process that was also voltage-dependent.

Channel conductance

The averaged conductance measured in α-chymotrypsin-modified channels (18.1 ± 2.5 pS) was not statistically different from non-modified Na^+ channels (16.3 ± 1.9 pS). The results suggest that the brief treatment of Na^+ channels with α-chymotrypsin as used in these experiments did not alter the activation kinetics or the permeation properties of the channel, and appeared to remove primarily the fast inactivation process (Patlak and Horn, 1982; Sheets and Hanck, 1993). Our results differ somewhat from those obtained during experiments requiring long and continued exposure to the enzyme as seen during whole-cell measurements in guinea pig ventricular myocytes (Clarkson, 1990). After more prolonged exposure to the enzyme, a shift of the I-V relationship is observed as well as an increase in Na^+ current. Sheets and Hanck (1993) observed only a slight increase (16%) in whole cell Na^+ current after dialysis of canine Purkinje cells with α-chymotrypsin. Our results extend their work and that of Clarkson (1990) by showing that the increase in macroscopic Na^+ current does not result from an increase single channel conductance. A part of the increase seen in earlier studies may have resulted from the observed shift of the activation curve caused by prolonged exposure to the enzyme. However, Sheets and Hanck (1993) have nicely shown that the observed shift of the activation curve resulted entirely from the time dependent changes that occur upon whole cell dialysis. In our study with excised patches, the time of exposure to the α-chymotrypsin action was much shorter (2–5 min) and caused no shift of the gating parameters. This supports their interpretation. The additional effects caused by prolonged enzyme exposure in the whole-cell mode could results from a greater degree of proteolysis as the enzyme has time to react with less accessible regions of the channel (Zwerling et al., 1991). This is expected to occur at any exposed regions that contain a preferred amino acid substrate sequence for α-chymotrypsin. The only additional basis for selectivity of α-chymotrypsin is the accessibility of the cleavage sites (Zwerling et al., 1991); brief exposure times such as we have used would only permit the most accessible sites to be attacked. Access to the "fast inactivation gate" is expected to occur easily, since the approximately 60 amino acids linking domains III and IV of the channel (III-IV linker) is a putative extramembranous, intracellular domain.

α-chymotrypsin is an endopeptidase that is specific for peptide bonds where the carboxyl terminal residue is con-

tributed by tyrosine, tryptophan or phenylalanine (Tyr-X, Phe-X, or Tryp-X). Vassilev et al. (1989) have demonstrated that antibodies directed toward the intracellular peptide segment connecting domains III and IV (the III-IV linker) can disrupt channel inactivation. Stühmer et al. (1989) demonstrated that mutations in this region altered channel inactivation. Potential sites for α-chymotrypsin cleavage in the cardiac III-IV linker region, are phenylalanine 1487 and the tyrosines at position 1495 and 1496 and 1518. Very recently, West et al. (1992) have demonstrated the phenylalanine equivalent to 1487 of the rat brain Na^+ channel isoform is important for inactivation.

Channel gating

Figures 5 and 6 indicate the voltage dependence of the open times. We observed that the channel open durations were prolonged as membrane potential was made less negative. There has been controversy as to whether the open times of cardiac Na^+ channels with intact fast inactivation are voltage-dependent. Nilius (1988) has concluded that the open times were not voltage-dependent, whereas Grant and Starmer (1987), Yue et al. (1989) and Berman et al. (1989) have provided evidence that they are voltage-dependent. Our own data show a small voltage dependence of the open times for channels where inactivation is intact, and this can be explained entirely by the voltage dependence of the closing rate (see Fig. 6 *A*). We considered the possibility that the observed voltage dependence of the open times in our experiments was an artifact caused by limited recording bandwidth or inappropriate threshold detection for opening and closing. If brief closures were observed at low voltages but became briefer and were increasingly missed at stronger depolarization, then open times that did not change with voltage would appear to become longer because brief closures would be missed. In this case, two shorter openings would be counted as one longer opening. We explored the latter possibility by re-measuring the open times using criteria of excursions of 3 and 4 SD from the mean open level. This would be more likely to detect brief closures that did not fully reach the 50% level and therefore would have gone undetected. Although this method gave more openings that were briefer, the voltage dependence was still apparent and the detected closures did not become briefer with greater membrane potential steps which indicates that the voltage dependence is not simply a measurement artifact. Also, missed closures could not account for the decrease in open times that was observed at positive membrane potentials.

If open channels can directly enter another state or enter the slow inactivated state then after removal of fast inactivation there is still more than one pathway from the open state. Zilberter and Motin (1991) have suggested the existence of two fast inactivated states detected by a two-stage action of trypsin. Our data show that after α-chymotrypsin the channels behave like the stage II that they describe. Therefore, the intermediate (stage I) proteolysis that they described was not observed by us using α-chymotrypsin. Since the open times are equal to the reciprocal sum of the rate constants leaving the open state, our estimates of the closing rate constant (β) will be in error to the extent that the rate constant for transition into the another inactivated state is of similar magnitude as the closing rate constant. This also could give rise to the non-log-linear plot of the reciprocal open times (Fig. 6). We do not believe this is the case, however, because these rate constants must differ by more than an order of magnitude, since there is no perceptible inactivation of the ensemble average during the test pulse shown in Figs. 7 and 8. Hence, the channel is much more likely to close or remain open ($C \rightleftharpoons O$) than to enter the slow inactivated state within a few hundred milliseconds. If for the sake of argument, we assume that 3% slow inactivation has occurred undetected during 50 millisecond, then an upper limit ($A/A_0 = e^{-50\cdot(\gamma si+\delta si)}$; $(\gamma_{si}+\delta_{si}) = -\ln(0.97)/50 = 0.6$ s^{-1}) can be placed on the rate constant for entering the slow inactivated state. Neither rate constant can be larger than 0.6 s^{-1}. This simplified calculation assumes a first order 2-state interaction with the slow inactivated state (reasonable provided that the rate constants for open-closed transition ($C \rightleftharpoons O$) and the rate constants for slow inactivation are greatly different). Since the sum of the two rate constants approximates the reciprocal of slow inactivation time constant ($1/\tau_{si} = (\gamma_{si}+\delta_{si}) = \sim 0.6$ s^{-1}), an estimate of the apparent time constant for slow inactivation is ~1.6 s near 0 mV, which is similar to that observed by Clarkson (1990). The rate constants for entering or leaving the slow inactivated state ($1/\tau_{si} = (\gamma_{si}+\delta_{si}) = \sim 0.6$ s^{-1}) must be much smaller than the rate constant for closing (2000–300 s^{-1}) and thus the open times largely reflect this single closing rate constant. This also places limits on the rate constant for fast inactivation. When fast inactivation is intact the open times are shorter because of the contribution from the rate constant (γ_{fi}) into the fast inactivated state (e.g., $\tau^{-1}_{open} = \beta + \gamma_{fi}$). With fast inactivation intact, open times range between 0.3 and 1.5 ms (Nilius, 1988; Kunze et al, 1985; Grant and Starmer, 1987) over the range of potentials we have explored (see Fig. 6). This suggests that the rate constant for entry into the fast inactivated state (γ_{fi}) must be on the order of 400 s^{-1}. This value gives open times of 0.4 to 1.4 ms over the range of membrane potentials we have examined (see Fig. 6*A*, *dashed lines*). It also produces macroscopic currents with appropriate kinetics over this range of membrane potentials. While our data do not address whether the fast inactivation rate constant is voltage-dependent, a minimal voltage dependence of this rate constant is consistent with known molecular features of the channel. The fast inactivation rate constant (γ_{fi}) is not expected to be very voltage dependent if it describes movement of a part of the channel protein, (e.g., III-IV linker domain) that is not in the electrical field (Armstrong and Bezanilla, 1977; Stühmer et al., 1989). Even so, the open times can show a moderate voltage dependence because of the contribution from the closing rate constant (β) which is voltage-dependent (see Fig. 6, *dashed lines*).

The voltage dependence of the channel open times suggest that closing of the channel requires movement of a charge or

dipole. The nonlinear nature of the logarithmic voltage dependence of the closing rate constant suggest that membrane field-induced dipoles may also influence gating (Stevens, 1978). A nonlinear voltage dependence has been observed in gating of end plate ACh channels of *Rana temporia* (Anderson and Stevens, 1973) and in mammalian potassium channels (Balser et al., 1990). The theoretical basis for such a voltage dependence of rate constants is discusses in detail by Stevens (1978).

Since gating of the channel presumably involves a rearrangement of atoms in the protein, the structure(s) responsible must sense the membrane field strength. Thus, it must achieve sufficient energy from thermal motion or other sources to traverse the energy barrier that separates the open and closed states. We estimated the height of this barrier from reaction rate theory. The activation energy for the closing reaction ranged between 13 and 14 kcal/mol over this range of membrane potentials as indicated by the dotted curve in Fig. 6 *B*. These values are similar to the barrier heights obtained for a gating transition of the *Drosophila A* channel (Zagotta and Aldrich, 1990).

Slow inactivation is not removed by α-chymotrypsin

Figures 7 and 9 indicate that prolonged closures occur after α-chymotrypsin modification. If internal proteolysis removes fast inactivation and leaves slow inactivation intact, then this suggests that these two processes are distinct and involve different domains in the Na^+ channel structure. These results allow us to rule out certain models for slow inactivation. Because slow inactivation remains after removal of fast inactivation, the channel must be able to enter the slow inactivated state(s) without having to pass through the fast inactivated state(s).

$$C_n \leftrightarrows C \leftrightarrows O \leftrightarrows I_{fast} \leftrightarrows I_{slow}$$

Scheme A

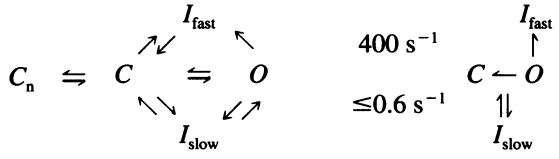

Scheme B

In Scheme A, channels first enter the fast inactivated state followed by a much slower transition into the slow inactivated state. In this case removal of the pathway into the fast inactivated state would also eliminate slow inactivation. In Scheme B, open channels can enter either the fast or the slow inactivated state. This is similar to the model proposed by Rudy (1978) for slow inactivation in *Myxicola* axons. In his model, channels would preferentially enter the fast inactivated state unless extremely long depolarizations (or very rapid stimulations) occurred. Only a small fraction of the channels would normally enter the slow inactivated state. For simplicity transitions between fast and slow inactivated states have been omitted from Scheme B; however, these transitions must also exist because it is possible to induce slow inactivation after the channels have undergone fast inactivation. This model is simplified on the right (Scheme B) with an estimate of the rate constant for fast inactivation from the open state. We can place limits on the magnitude of the slow inactivated state interactions, in that we know the aggregate of the rate constants involved must be smaller than about 0.6 s^{-1}. The fact that we cannot resolve the exact transition rate constants is indicated by the imprecise location of the arrows leading to the slow inactivated state. Our data are also consistent with a competition between the fast and slow inactivation process. After enzymatic modification, the likelihood of null sweeps was increased, presumably because after removal of fast inactivation the channel could more readily enter a long-lived slow inactivated state. When fast inactivation was intact, channels would typically open once and become fast inactivated. We never observed large numbers of consecutive null records in control experiments as we did after remove of fast inactivation. Under control conditions, channels almost always opened at least once upon depolarization: only 11 of the 96 (12%) records used to create the ensemble average in Fig. 2 were nulls. After removal of fast inactivation, 41 of 128 records (32%) had no openings. This can account for the observation that the ensemble current is of similar magnitude before and after removal of fast inactivation. If fast inactivation is intact, the large rate constant (400 s^{-1}) for entry into the fast inactivated state dominates the reaction (γ_{si} < 1 s^{-1}) and channels would infrequently enter the slow inactivated state. After removal of fast inactivation, channels can more readily enter the slow inactivated state, since there is no competition from the fast inactivated state.

We thank Drs. D. Roden, D. Snyders, L. Hondeghem, J. Tamargo, and E. Delpón for reading and critique of the manuscript, and Craig Short for technical assistance.

This work was supported by the National Institutes of Health Grants HL40608, HL46681, and HL51197. Dr. Valenzuela was a recipient of an International Fellowship from the Fulbright Foundation. P. Bennett is an Established Investigator of the American Heart Association.

REFERENCES

Aldrich, R. W., D. P. Corey, and C. F. Stevens. 1983. A reinterpretation of mammalian sodium channel gating based on single channel recording. *Nature.* 306:436–441.

Anderson, C. R., and C. F. Stevens. 1973. Voltage clamp analysis of acetylcholine produced end-plate current fluctuations at the frog neuromuscular junction. *J. Physiol. (Lond.)* 235:655–691.

Armstrong, C., and F. Bezanilla. 1977. Inactivation of the sodium channel. II. Gating current experiments. *J. Gen. Physiol.* 70:567–590.

Armstrong, C., F. Bezanilla, and E. Rojas. 1973. Destruction of sodium inactivation in squid axons perfused with pronase. *J. Gen. Physiol.* 62: 375–391.

Bean, B. 1981. Sodium channel inactivation in the crayfish giant axon. Must channels open before inactivating? *Biophys. J.* 35:595–614.

Bendat, J. S., and A. G. Piersol. 1986. Random Data: Analysis and Measurement Procedures, 2nd Ed. John Wiley and Sons, New York. 95–97.

Berman, M. F., J. S. Camardo, R. B. Robinson, and S. A. Siegelbsum. 1989. Single sodium channels from canine ventricular myocytes: voltage dependence and relative rates of activation and inactivation. *J. Physiol.* 415:503–531.

Bezanilla, F., and C. Armstrong. 1977. Inactivation of the sodium channel. I. Sodium current experiments. *J. Gen. Physiol.* 70:549–566.

Brown, A., K. Lee, and T. Powell. 1981. Sodium current in single rat heart muscle cells. *J. Physiol.* 318:479–500.

Catterall, W. 1986. Molecular properties of voltage-sensitive sodium channels. *Annu. Rev. Biochem.* 55:953–985.

Catterall, W. 1988. Structure and function of voltage-sensitive ion channels. *Science.* 242:50–61.

Clarkson, C. 1990. Modification of Na^+ channel inactivation by α-chymotrypsin in single cardiac myocytes *Pflügers Arch.* 417:48–57.

Clarkson, C., T. Matsubara, and L. Hondeghem. 1984. Slow inactivation of $\dot{V}_{max}$ in guinea-pig ventricular myocardium. *Am. J. Physiol.* 16:645–654.

Colquhoun, D., and F. Sigworth. 1983. Fitting statistical analysis of single-channel records. *In* Single-Channel Recordings. B. Sakmann and E. Neher, editors. Plenum Press, New York. 191–263.

Cota, G., and C. M. Armstrong. 1989. Sodium channel gating in clonal pituitary cells. *J. Gen. Physiol.* 94:213–232.

Farmer, B., M. Mancina, E. Williams, and A. Watanabe. 1983. Isolation of calcium tolerant myocytes from adult rat heart: review of the literature and description of a method. *Life Sci.* 33:1–18.

Fozzard, H. A., and D. A. Hanck. 1992. Sodium Channels. *In* The Heart and Cardiovascular System, Vol 1, Ch. 41. H. A. Fozzard, E. Haber, R. Jennings, A. Katz, H. Morgan, editors. Raven Press, New York. 1091–1119.

Fozzard, H. A., C. T. January, and J. C. Makielski. 1985. New studies of the excitatory sodium currents in heart muscle. *Circ. Res.* 56:475–485.

Gillespie, J., and H. Meves. 1980. The time course of sodium inactivation in squid giant axons. *J. Physiol. (Lond.).* 299:289–307.

Gintant, G., N. Datyner, and I. Cohen. 1984. Slow inactivation of a tetrodotoxin-sensitive current in canine cardiac Purkinje fibers. *Biophys. J.* 45:509–512.

Goldman, L., and C. Schauf. 1972. Inactivation of the sodium current in *Myxicola* giant axons. Evidence for coupling to the activation process. *J. Gen. Physiol.* 59:659–675.

Gonoi, T., and B. Hille. 1987. Gating of Na^+ channels. Inactivation modifiers discriminate among models. *J. Gen. Physiol.* 89:253–274.

Grant, A. O., and C. F. Starmer. 1987. Mechanisms of closure or cardiac sodium channels in rabbit ventricular myocytes: single-channel analysis. *Circ. Res.* 60:897–913.

Hamill, O., A. Marty, E. Neher, B. Sakmann, and F. Sigworth. 1981. Improved patch-clamp techniques for high-resolution current recording from cells and cell-free membrane patches. *Pflügers Arch.* 391:85–100.

Hille, B. 1992. The Ionic Channels of Excitable Cells. Sinauer, Sunderlan, MA.

Hodgkin, A., and A. Huxley. 1952. A quantitative description of membrane current and its application to conduction and excitation in nerve. *J. Physiol.* 117:500–544.

Isenberg, G., and U. Klöckner. 1982. Calcium tolerant ventricular myocytes prepared by preincubation in a "KB-medium." *Pflügers Arch.* 395:6–18.

Kirsch, G., and A. Brown. 1989. Kinetic properties of single sodium channels in rat heart and rat brain. *J. Gen. Physiol.* 93:85–99.

Kunze, D., A. Lacerda, D. Wilson, and D. Brown. 1985. Cardiac Na^+ currents and the inactivating, reopening, and waiting properties of single cardiac Na^+ channels. *J. Gen. Physiol.* 86:691–719.

Lawrence, J. H., D. T. Yue, W. C. Rose, and E. Marban. 1991. Sodium channel inactivation from resting states in guinea-pig ventricular myocytes. *J. Physiol.* 443:629–650.

Moorman, J. R., G. E. Kirsch, A. M. Brown, and R. H. Joho. 1990. Changes in sodium channel gating produced by point mutations in a cytoplasmic linker. *Science.* 250:688–691.

Nilius, B. 1988. Modal gating behavior of cardiac sodium channels in cell-free membrane patches. *Biophys. J.* 53:857–862.

Noda, M., I. Ikeda, T. Kayano, H. Suzuki, H. Takeshima, H. Kurasaki, H. Takahashi, and S. Numa. 1986. Existence of distinct (sodium channel) messenger RNAs in rat brain. *Nature.* 320:188–192.

Noda, M., S. Shimizu, T. Tanabe, T. Takai, T. Kayano, T. Ikeda, H. Takahashi, H. Nakayama, Y. Kanaoka, N. Minamino, K. Kangawa, H. Matsuo, M. Raftery, T. Hirose, S. Inayama, H. Hayashida, T. Miyata, and S. Numa. 1984. Primary structure of *Electrophorus electricus* sodium channel deduced from $cDNa^+$ sequence. *Nature.* 312:121–127.

Oxford, G. 1981. Some kinetic and steady-state properties of sodium channels after removal of inactivation. *J. Gen. Physiol.* 77:1–22.

Patlak, J., and R. Horn. 1982. Effect of N-bromoacetamide on single sodium channel currents in excised membrane patches. *J. Gen. Physiol.* 79: 333–351.

Patlak, J., and M. Ortiz. 1985. Slow currents through single sodium channels of the adult rat heart. *J. Gen. Physiol.* 86:89–104.

Quandt, F. 1987. Burst kinetics of sodium channels which lack fast inactivation in mouse neuroblastoma cells. *J. Physiol. (Lond.).* 392:563–585.

Rogart, R. B., L. L. Cribs, L. K. Muglia, D. D. Kephart, and M. W. Kaiser. 1989. Molecular cloning of a putative tetrodotoxin resistant rat heart Na^+channel isoform. *Proc. Natl. Acad. Sci. USA.* 86:8170–8174.

Rudy, B. 1978. Slow inactivation of the sodium conductance in squid giant axons. Pronase resistance. *J. Physiol.* 283:1–21.

Rudy, B. 1981. Inactivation in *Myxicola* giant axons responsible for slow and accumulative adaption phenomena. *J. Physiol.* 312:531–540.

Saikawa, T., and E. Carmeliet. 1982. Slow recovery of the maximal rate of rise ($\dot{V}_{max}$) of the action potential in sheep cardiac Purkinje fibers. *Pflügers Arch.* 394:90–93.

Scanley, B. E., D. A. Hanck, T. Chay, and H. A. Fozzard. 1990. Kinetic analysis of single sodium channels from canine cardiac Purkinje cells. *J. Gen. Physiol.* 95:411–435.

Sheets, M. F., and D. A. Hanck. 1993. Modification of sidium channel inactivation by α-chymotrypsin in canine cardiac Purkinje cells. *J. Cardiovasc. Electrophysiol.* 4:686–694.

Stevens, C. F. 1978. Interactions between intrinsic membrane proteins and electric fields. *Biophys. J.* 22:295–306.

Stühmer, W., F. Conti, H. Suzuki, X. Wang, M. Noda, N. Yahagi, H. Kubo, and S. Numa. 1989. Structural parts involved in activation and inactivation of the sodium channel. *Nature.* 339:597–603.

Valenzuela, C., and P. B. Bennett. 1991. Voltage- and use-dependent modulation of the calcium current by amiodarone and des-oxo-amiodarone. *J. Cardiovasc. Pharmacol.* 17:894–902.

Vandenberg, C., and R. Horn. 1984. Inactivation viewed through single sodium channels. *J. Gen. Physiol.* 84:535–564.

Vassilev, P., T. Scheuer, and W. A. Catterall. 1989. Inhibition of inactivation of single Na^+ channels by a site directed antibody. *Proc. Natl. Acad. Sci. USA.* 86:8147–8152.

West, J. W., D. E. Patton, T. Scheuer, Y. Wang, A. L. Goldin, and W. A. Catterall. 1992. *Proc. Natl. Acad. Sci. USA.* 89:10910–10914.

Yue, D. T., J. H. Lawrence, and E. Marban. 1989. Two molecular transitions influence cardiac sodium channel gating. *Science.* 244:349–352.

Zagotta, W. N., and R. W. Aldrich. 1990. Voltage-dependent gating of *Shaker A*-type potassium channels in *Drosophila* muscle. *J. Gen. Physiol.* 95:29–60.

Zilberter, Y. I., and L. G. Motin. 1991. Existence of two fast inactivated states in cardiac Na channel confirmed by two stage action of proteolytic enzymes. *Biochim. Biophys. Acta.* 1068:77–80.

Zwerling, S. J., S. A. Cohen, and R. L. Barchi. 1991. Analysis of protease-sensitive regions of the skeletal muscle sodium channel in vitro and implications for channel tertiary structure. *J. Biol. Chem.* 266:4574–4580.